JACS
JOURNAL OF THE AMERICAN CHEMICAL SOCIETY

ARTICLE

pubs.acs.org/JACS

Cathode Composites for Li−S Batteries via the Use of Oxygenated Porous Architectures

Rezan Demir-Cakan,[†,‡] Mathieu Morcrette,[†,‡] Farid Nouar,[§] Carine Davoisne,[†] Thomas Devic,[§] Danielle Gonbeau,[∥,‡] Robert Dominko,[‡,⊥] Christian Serre,[§] Gérard Férey,[§] and Jean-Marie Tarascon*[,†,‡]

[†]LRCS, UMR CNRS 6007, Université de Picardie Jules Verne, 33 Rue Saint-Leu, 80039 Amiens cedex, France

[‡]ALISTORE-ERI, 80039, 33 Rue Saint-Leu, Amiens, France

[§]Institut Lavoisier, UMR CNRS 8180, Université de Versailles Saint-Quentin-en-Yvelines, 45 avenue des Etats-Unis, 78035 Versailles cedex, France

[∥]IPREM-ECP, UMR CNRS 5254, Université de Pau et des Pays de l'Adour, 2 avenue P. Angot, 64053 Pau, France

[⊥]National Institute of Chemistry, Hajdrihova 19, SI-1000 Ljubljana, Slovenia

Supporting Information

ABSTRACT: Li−S rechargeable batteries are attractive for electric transportation because of their low cost, environmentally friendliness, and superior energy density. However, the Li−S system has yet to conquer the marketplace, owing to its drawbacks, namely, soluble polysulfide formation. To tackle this issue, we present here a strategy based on the use of a mesoporous chromium trimesate metal−organic framework (MOF) named MIL-100(Cr) as host material for sulfur impregnation. Electrodes containing sulfur impregnated within the pores of the MOF were found to show a marked increase in the capacity retention of Li−S cathodes. Complementary transmission electron microscopy and X-ray photoelectron spectroscopy measurements demonstrated the reversible capture and release of the polysulfides by the pores of MOF during cycling and evidenced a weak binding between the polysulphides and the oxygenated framework. Such an approach was generalized to other mesoporous oxide structures, such as mesoporous silica, for instance SBA-15, having the same positive effect as the MOF on the capacity retention of Li−S cells. Besides pore sizes, the surface activity of the mesoporous additives, as observed for the MOF, appears to also have a pronounced effect on enhancing the cycle performance. Increased knowledge about the interface between polysulfide species and oxide surfaces could lead to novel approaches in the design and fabrication of long cycle life S electrodes.

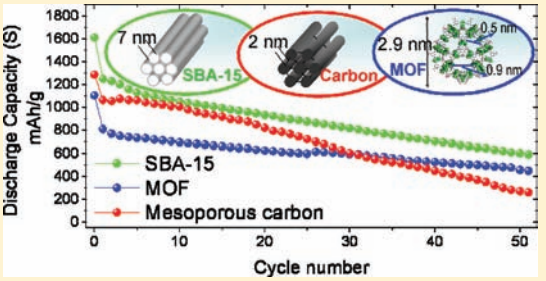

INTRODUCTION

Developing batteries for load leveling and transport is still a formidable challenge, especially for materials chemistry, and will be a major focus of endeavor for years to come. The rechargeable lithium-ion (Li-ion) battery is regarded as the device of choice for the near future because of its higher energy density compared to other rechargeable batteries, enabling the development of smaller and lighter batteries that can store more energy. However, even Li-ion batteries will not be able to store sufficient energy for the extended driving range required by electric vehicles in the long term, therefore we need to explore new batteries that are different from Li-ion and offer a real step change in energy storage.

Within this context, Li−S batteries could be a viable option since they effectively possess higher theoretical specific energy over conventional Li-ion batteries, assuming complete reaction of Li and S to form Li_2S (2600 Wh/kg or 2800 Wh/l) and present cost, environmental, and sustainable attributes. Although studies on the Li−S system were initiated back to the early 60s,[1] the system has yet to conquer the marketplace, as a few scientific hurdles remain to be cleared. Among them are: (i) the use of a Li metal anode which brings safety problems,[2] (ii) the low active material utilization due to the insulating nature of both the sulfur itself and the polysulfide species resulting from its reduction, and (iii) the poor electrode cyclability, owing to the solubility in various electrolytes of the polysulfides generated during the battery operation.[3]

Past research efforts have been devoted to address these issues. For instance, modifying electrolyte formulation via additives in order to form a protective surface film for Li electrode[4] or using polymers[5] rather than liquid-type electrolytes was attempted to restrain the polysulfides solubility. Besides, several approaches were pursued to prepare highly electronic conducting, porous C/S composites in order to capture polysulfide species within the electrode configuration. Among the most elegant ones is Nazar's approach[6] which relies on the use of ordered mesoporous carbon composite so as to provide both an electronic percolation path through the electrode and an adequate controlled porosity to

Received: July 6, 2011
Published: September 01, 2011

retain part of the electrochemically generated polysulfides species. Although such a structural electrode design has led to pronounced electrochemical performances in terms of capacity retention, it is still insufficient for practical applications. There are still a few soluble species escaping from the carbon channels, leading to a consequent capacity loss upon several cycles. Consequently, finding enhanced confined environment is a crucial point to obtain better cycling capability over numerous cycles.

Here, we propose to use a metal−organic framework (MOF) as an improved confined matrix for sulfur impregnation. In the field of electrode materials, the successful use of MOFs is already proven through either the mixed valence metallic centers[7] or the redox active organic linkers.[8] Insertion of redox active species into the pores of MOFs was also studied in order to improve the performance.[9] MOFs have also been considered for the encapsulation of dense inorganic species, such as metals,[10] oxides,[11] hydrides[12] or even drug deliveries.[13] For such applications, the chemical stability of the MOFs is of utmost importance. This characteristic is known to be highly dependent on their chemical composition.[14,15] In this prospect, we focused our attention on the chromium trimesate MIL-100(Cr)[16] (MIL: Materiaux Institut Lavoisier), a highly porous solid and a hydrothermally stable MOF whose reasonable stability under high pressure of H_2S has already been established.[17] This solid is built up from oxocentered trimers of chromium octahedra linked with 1,3,5-benzentricarboxylate ligands defining hybrid super tetrahedral motifs, which are further connected to define an expanded zeolitic structure. It consists of two types of mesoporous cages (∼25−29 Å) connected through microporous pentagonal (∼5 Å) and hexagonal windows (∼9 Å) (Figure S1 in Supporting Information). With its large pore volume (∼ 1 $cm^3\ g^{-1}$) and small windows limiting the diffusion processes, this compound appears as a suitable candidate for the encapsulation of sulfur and its corresponding reduced state species.

Despite its unique mesoporous structure, with pores being able to host some liquid electrolyte providing high ionic conductivity through the electrode, the MIL-100(Cr) has an insulating nature which would suggest, at first glance, avoiding its utilization for sulfur impregnation. However, past studies on insulating host materials, i.e., $LiFePO_4$, taught us that its electrochemical activity can be triggered by the use of carbon conducting coatings[18,19] which enables the proper electrode wiring. At this stage, it should be recalled that in Li−S batteries, the S electrolyte can be viewed as a catolyte despite the fact that the starting sulfur is a solid powder; the reason being that S transforms into soluble polysulfide during the first reduction and never returns to elemental sulfur upon successive cycles. Therefore, these polysulfide species are prone to move outward the confined electrode. This is why it is often claimed that the confinement effect caused by the use of a nanoporous self-supporting S matrix is more important than its conductivity. This was another impetus to prepare MOF/S composites.

Herein, sulfur was infiltrated within the pores of MIL-100(Cr) using the melt diffusion concept,[6] i.e., the MIL-100(Cr) and the sulfur were mixed at room temperature and then heated to 155 °C. The resulting solid was labeled as MIL-100(Cr)/S@155.

EXPERIMENTAL SECTION

Synthesis of the Composites. The synthesis and activation of the MIL-100(Cr) are described elsewhere.[16]

The synthesis of the MIL-100(Cr)/S@155 composite was performed following a melt-diffusion strategy.[6] First, the MIL-100(Cr) (which was degassed at 170 °C prior to use) and the sulfur were mixed together and placed in a crucible, the mixture was then heated to 155 °C with a 0.2 °C/min heating ramp, and no additional washing procedure was applied afterward. The ratio between sulfur and MIL-100(Cr) was precisely adjusted considering the density of liquidized sulfur (1.82 g/cm^3) and the pore volume of the MIL-100(Cr) (0.95 cm^3/g) as well as the need for free surface volume for volume expansion of the lithiated sulfur. The density of sulfur (2.07 g/cm^3) is higher than Li_2S (1.66 g/cm^3). According to the nitrogen sorption analysis, the free volume of the MIL-100(Cr)/S@155 is 0.18 g/cm^3. Prior to being used as an electrode material, the MOF/S composite was ball milled with different amounts of carbon (12.5, 25, and 50%) at 300 rpm for 15 min. According to thermogravimetric and energy-dispersive spectrometry (EDS) analyses, the MIL-100(Cr)/S@155 composite contains ∼48 wt % sulfur. Thermogravimetric analysis calculation is based on the fact that MIL-100(Cr) also starts to decompose above 250 °C.

The synthesis of the Mesoporous carbon/S@155 composite was performed in a similar fashion. The SBA-15 template was first synthesized according to the method described by Stucky et al.[20] After synthesis, the pores of the SBA-15 template were completely filled with an aqueous solution of sucrose/H_2SO_4. The resulting wet sucrose/SBA-15 was calcined at 900 °C under inert atmosphere. The silica was thereafter removed from the composites using a 4 M aqueous solution of ammonium hydrogen difluoride yielding carbon replicas. The mesoporous carbon and sulfur were then ground together at room temperature and heated to 155 °C. The carbon/sulfur composite after impregnation at 155 °C has 52 wt % sulfur, according to thermogravimetric analysis (TGA) analysis (data not shown).

The same procedure was also applied to the preparation of the SBA-15/S composites through sulfur impregnation at 155 °C. According to TGA analysis, the composite after impregnation at 155 °C contains 50 wt % of sulfur. Prior to being used as an electrode material, the composite was ball milled with different amounts of carbon (12.5, 25, and 50%) at 300 rpm for 15 min.

Characterizations. The X-ray powder diffraction patterns of the solids were recorded on a Bruker D8 Advance diffractometer ($\theta-2\theta$ mode, Co Kα radiation λ = 1.7903 Å, and a linear position-sensitive detector).

The microstructural and chemical analyses were done using a transmission electron microscope (TEM-FEI TECNAI F20 S-TWIN) fitted with a scanning mode and both high-angle annular dark-field (HAADF) detector and EDAX EDS.

The BET surface area and pore volume of the solids were evaluated by nitrogen sorption at 77K using a Micromeritics ASAP2020 apparatus. Note that for the sulfur impregnated samples, no degassing procedure was applied prior to the measurement due to the low melting point of sulfur (115 °C) as opposed to their parent material, which was degassed at 150 °C for 6 h.

TGAs were performed on a Netzsch STA 449 "Jupiter" apparatus, between the room temperature and 500 °C under flowing Ar (25 mL/min) at a 5 K/min heating rate.

Calorimetric measurements were carried out by Differential Scanning Calorimetry (Netzsch DSC 204) under argon flow (100 mL/min), using aluminum crucibles and a heating rate of 5 °C/min.

X-ray photoelectron spectroscopy (XPS) measurements were carried out with a Kratos Axis Ultra spectrometer, using a focused monochromatized Al Kα radiation (hν = 1486.6 eV). The spectrometer was calibrated using the photoemission line $Ag3d_{5/2}$ (binding energy 368.3 eV). Spectra were recorded with 20 eV constant pass energy. The analyzed area of the samples was 300 × 700 μm^2, charge neutralization was used, and the pressure in the analysis chamber was ca. 5×10^{-7} Pa. Short-time spectra were recorded before and after each experiment and compared to check the nondegradation of the samples in the X-ray beam. The binding energy (BE) scale was calibrated from the carbon contamination

using the C1s peak at 285.0 eV. Peak positions and areas were obtained by a weighted least-squares fitting of model curves (70% Gaussian, 30% Lorentzian) to the experimental data. Quantification was performed on the basis of Scofield's relative sensitivity factors.

Electrochemistry. Experiments were carried out using two-electrode Swagelok-type cells. The MOF/S and SBA-15/S electrodes were prepared by mixing the composites with 12.5, 25, or 50 wt % of Ketjen black carbon (as conductor) with ball milling. The mesoporous carbon/S composite was hand milled with 20 wt % of additional Ketjen black carbon (as conductor). The glass fiber (GF/D) from Whatman was used as a separator, and pure lithium foil (Aldrich) was used as counter electrode. The electrolyte consisted of a solution of 1 M of lithium bis(trifluoromethane sulfone)imide ($LiN(SO_2CF_3)_2$) (LiTFSI) containing a tetramethylene sulfone (TMS) electrolyte solution at a current density of C/10 with the voltage values ranging from 1.0 to 3.0 V. The cells were assembled inside an argon-filled glovebox.

Electrochemistry in four-electrode cells was tested simultaneously on two channels using galvanostat/potentiostat VMP2 (Biologic, S.A., Claix, France). Prior to sulfur reduction, the cyclovoltamogram (CV) between stainless steel wire (working electrode) and lithium (reference and counter electrode) was measured with a scan rate of 0.3 mVs^{-1} over the 2.5−0.5 V voltage range versus metallic lithium. During this measurement the Li−S battery was on open circuit voltage (OCV) mode, and as soon as CV scan had been completed, the galvanostatic measurement of the Li−S battery was initiated for 2 h with a current density corresponding to C/20 cycling rate. Measurements were repeated in this sequence until the battery reached the cutoff voltage of 1.0 V versus metallic Li. Li foil and cathode composite (the mass of sulfur in all experiment was 5 mg) were positioned on each side of the separators. An OCV between stainless steel and lithium was typically 2.5 V. To exploit further the correlation between the amounts of charge of polysulfides, we performed integration of the peak in the voltage range from 2.25 to 1.5 V versus Li.

RESULTS AND DISCUSSION

X-ray powder diffraction (Figure 1a) indicates that the crystalline structure of the MOF remains intact, and no trace of crystalline sulfur is detected after impregnation at 155 °C (blue line pattern in Figure 1a). On the other hand, simple hand milling of the MIL-100(Cr) and sulfur at room temperature (abbreviated as MIL-100(Cr)/S@RT) resulted in a mixture of these two phases (red line pattern in Figure 1a). We can thus conclude that the sulfur impregnation of the MOF has been successfully achieved at 155 °C.

Additionally, in order to gain electronic wiring and uniform distribution of the conductive carbon, different amounts of carbon were ball milled with MOF/S composite at 300 rpm for 15 min. The green line pattern in Figure 1a shows that no amorphization of the MOF happened during the milling process. The nitrogen adsorption isotherms of the parent MIL-100(Cr) and the corresponding MIL-100(Cr)/S@155 composite prior to the ball milling process are shown in Figure 1. The insertion of sulfur leads to a strong decrease in the total pore volume (from 0.95 to 0.18 cm^3/g) and the BET surface area (1485 and 360 m^2/g in MIL-100(Cr) and MIL-100(Cr)/S@155, respectively) as well as a decrease in the overall pore size, as deduced from the disappearance of the adsorption mesoporous substep. This indicates that a large portion of the porosity is filled with sulfur.

TEM studies of MIL-100(Cr)/S@155 using HAADF-STEM combined with EDS analyses were used for the determination of the sulfur distribution throughout the MIL-100(Cr) matrix (Figure S2, Supporting Information). An EDS line profile

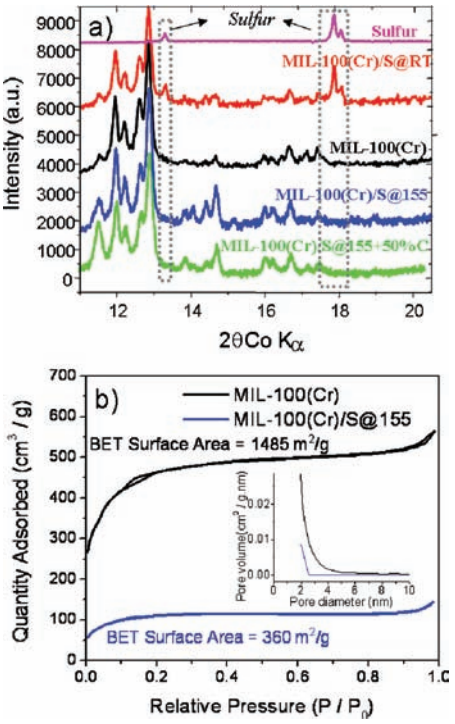

Figure 1. (a) X-ray diffraction patterns of sulfur, MIL-100(Cr) and resulting composites. (b) Nitrogen sorption isotherms of the MIL-100(Cr) and the sulfur containing composite (MIL-100(Cr)/S@155).

performed across a grain is shown in Figure S2a, Supporting Information (red line) and its chemical S/Cr ratio in Figure S2b, Supporting Information. The S/Cr ratio lessens on the border of the grain; this means that the sulfur is located inside the particle and depleted at the edges, further confirming the incorporation of sulfur in the matrix. Lastly, differential scanning calorimetric curves (Figure S3, Supporting Information) recorded in Ar atmosphere indicate the presence of exothermic sulfur melting point for the room temperature hand-milled sample as compared to its disappearance for the 155 °C treated sample. Besides suggesting some types of S interactions with the MOF matrix, this result confirms the conclusion drawn from XRD (Figure 1a) and TEM (Figure S2, Supporting Information) analyses, namely that a complete impregnation of sulfur into the MOF occurred upon heat treatment at 155 °C. Thermogravimetric (data not shown) and EDS analyses reveal that the whole composite, MIL-100-(Cr)/S@155, contains about 48 wt % of sulfur.

The lithium storage properties of the resulting materials are shown in Figure 2a and b. Galvanostatic discharge−charge experiments were carried out to evaluate the electrochemical performance of the MIL-100(Cr)/S@155 composite in the presence of different amounts of conductive carbon additives, namely 12.5, 25, and 50%. For comparison, the mesoporous hexagonally ordered carbon/sulfur composite as well as the MIL-100(Cr)/S@RT were tested. The discharge and charge curves for all composite electrodes were obtained in 1 M of LiTFSI containing a TMS electrolyte solution at a current density of C/10. Each cell was duplicated to ensure the robustness of our results. During the first discharge (Figure 2a), all composites show a staircase voltage profile independent of the composites; this is typical of Li−S system. At the upper plateau (2.3−2.4 V vs Li), elemental sulfur (S_8) accepts electrons leading to long-chain polysulfide anions

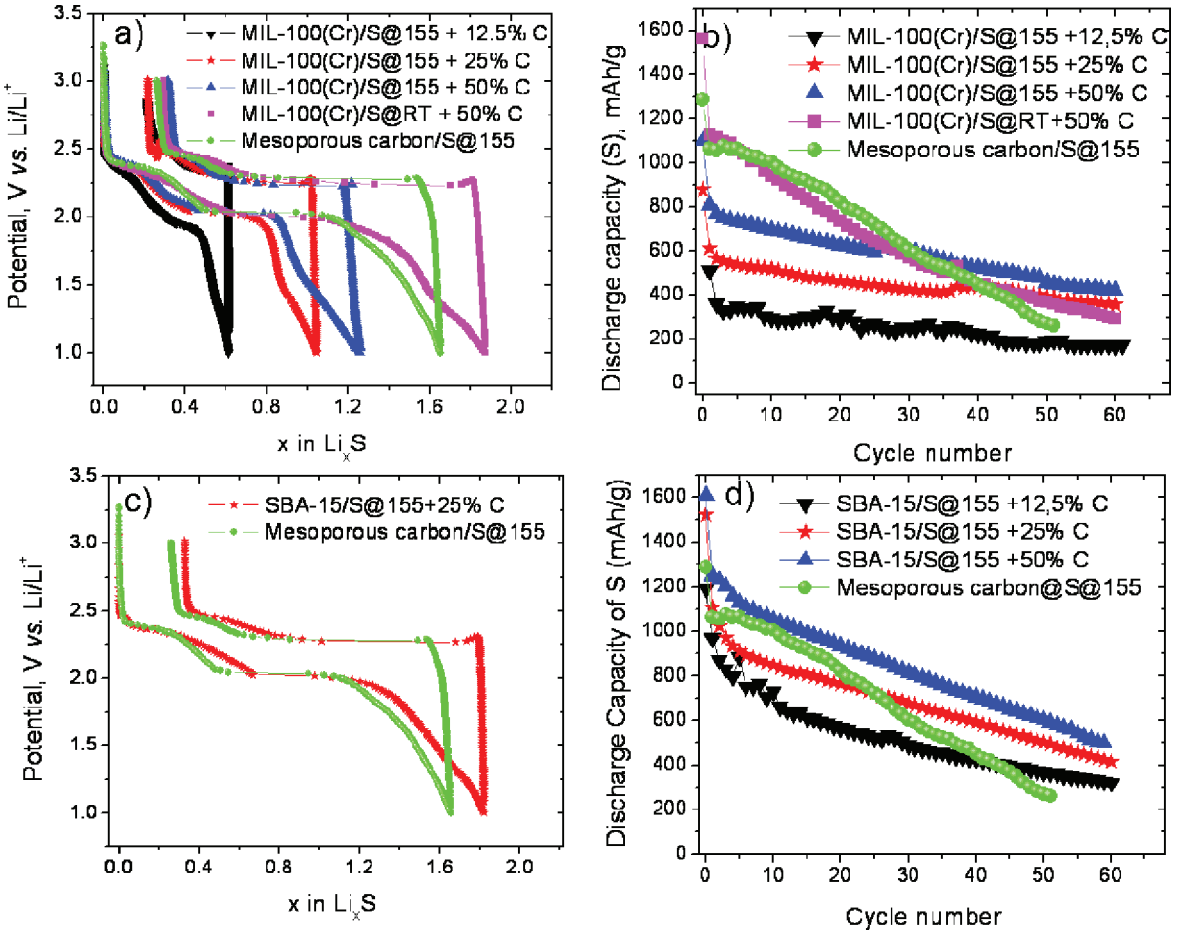

Figure 2. (a) First galvanostatic discharge/charge profiles of MIL-100(Cr)/S@155 composites with different conductive carbon additives, MIL-100(Cr)/S@RT and mesoporous carbon/S@155, at constant C/10 current density for the voltage range between 1.0 and 3.0 V vs Li (b) cycling performance of the MIL-100(Cr)/S@155 composites with different conductive carbon additives, MIL-100(Cr)/S@RT and mesoporous carbon/S@155. (c) First galvanostatic discharge/charge profiles of the SBA-15/S@155+ 25%C composite and mesoporous carbon/S@155 at constant C/10 current density for the voltage range between 1.0 and 3.0 V vs Li (b) cycling performance of the SBA-15/S@155 composites with different conductive carbon additives and mesoporous carbon/S@155 (the specific capacity was calculated by using the active material mass (sulfur) of the composites, given in mAh/g).

(e.g., Li_2S_8, Li_2S_6).[2] At the lower plateau (~2.0 V vs Li), further reduction takes place and forms the final solid product, Li_2S. In the case of MIL-100(Cr)/S@155, the polarization between the charge and discharge profiles decreases from 0.43 and 0.28 to 0.23 V in the presence of 12.5, 25, and 50 wt % carbon used, indicating the strong contribution of the conductive carbon additives, respectively. The MIL-100(Cr)/S@155/carbon composites show a reversible capacity retention at C/10 in the voltage range of 1−3 V vs Li, which is better than that measured for mesoporous carbon/S composites (Figure 2b). Li storage properties of MIL-100(Cr)/S@RT and MIL-100(Cr)/S@155 were also compared. Although MIL-100(Cr)/S@RT+50%C delivers very high discharge capacity (ca. 1580 mAh/g) (all the capacity calculation is based on the sulfur content of the composites given in mAh/g) during the first cycle, the capacity sharply decays in the following cycles (pink square in Figure 2b). We believe this is due to the sulfur particles, which are not inside the pore of MIL-100(Cr); thus, the nonembedded polysulfides species formed might easily diffuse throughout the electrode and deposit on the Li side where they are reduced, resulting overall in poorer capacity retention.

The structural benefit of the MOF over the mesoporous carbon is prominent (e.g., comparing blue triangle and green curves in Figure 2b), and this remarkably high capacity retention can be ascribed to the unique pore shape of MIL-100(Cr) (large pores but small windows), which essentially slows down the polysulfides diffusivity out of the 5−8.6 Å apertures of the windows. Moreover, the existence of polar parts due to the inorganic moieties in MIL-100(Cr) may provide further trapping function for the highly polar polysulfide species. A detailed XPS analysis of the MIL-100(Cr)/S@155 revealed that indeed a complex phenomenon (interaction/reactivity) occurs after sulfur impregnation. Figure 3a shows that the S2p peak of the typical sulfur powder corresponds to a well-resolved doublet (binding energy (BE): 164.3−165.5 eV). Upon impregnation of sulfur into MIL-100(Cr), the large majority of these sulfur atoms (88%) appears at a binding energy (163.9−165.1 eV) slightly different from the S2p BE of sulfur powder (164.3−165.5 eV) (Figure 3b). This BE shift can be associated with changes in the electronic distribution on the sulfur atoms in MIL-100(Cr)/S@155. However, the other part (12%) corresponds to sulfur atoms in a sulfate-like environment characterized by a very different BE (168.5−169.7 eV). It is also to be noted that fluorine content, which is present in the structure to provide charge balance (MIL-100(Cr) is formulated $Cr_3O(C9H_3O_6)2X$, where X = OH, F), is decreased at the

dx.doi.org/10.1021/ja2062659 |J. Am. Chem. Soc. 2011, 133, 16154–16160

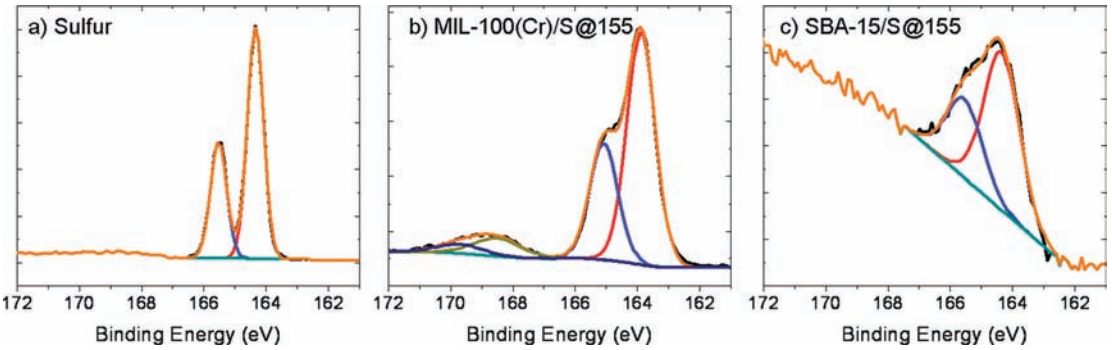

Figure 3. XPS analysis S2p spectrum of: (a) elemental sulfur, (b) MIL-100(Cr)/S@155 and (c) SBA-15/S@155.

surface after sulfur impregnation (Table S1 in Supporting Information), showing the partial replacement of fluorine by sulfate. Overall, these experiments give evidence for the presence of S interactions, which is not a total surprise with an element capable of easily clinging to metal surfaces. Whatever the nature of the S−MOF interaction, it could be: (i) at the origin of the DSC data (no S melting point peak was detected upon impregnation at 155 °C, Figure S3, Supporting Information) and (ii) responsible for a small shoulder at 1.5 V (vs Li) in Figure 2a. Further XPS results (Figure S4, Supporting Information) confirmed that the C1s, O1s, and Cr2p peaks are similar to the peaks of the host material. These results show that the sulfur impregnation does not involve any significant modification of the MIL-100(Cr) structure, as also proven by X-ray diffraction (Figure 1a).

It is evident that a high electronic conductivity carbon additive ensured good electrical contact among the nanometer-sized particles during Li insertion and extraction processes. A HAADF STEM image of MIL-100(Cr)/S@155 after the second cycle is presented in Figure S5a, Supporting Information. The whiter geometrical particles correspond to the MIL-100(Cr)/S@155 (Point 1) and the network surrounding them is the carbon additives (Point 2), according to the EDS analysis displayed in Figure S5b, Supporting Information. At Point 2, a diminutive fraction of sulfur was detected, meaning that during cycling, soluble polysulfides are removed from the pore matrix. Overall, these results confirm that Li−S batteries are based on an "all liquid" phenomenon in which soluble species could easily leave the pores and reach the electron conductive additives whatever the pore size of the confined matrices.

Although a few details remain to be clarified, the above results unambiguously show the positive attributes of using mesoporous MOF powders as host materials for sulfur impregnation as compared to conventional sulfur/mesoporous carbon composites, in terms of electrochemical performances, namely capacity retention. Therefore, at this stage a legitimate question is whether such an observed effect is specific to MOF or can it exist as well with other porous structures. To answer this question we decided to study the effect of sulfur impregnation into a mesoporous silica (SBA-15)[20] rather than in the MOF structure. Compared with mesoporous carbon, SBA-15 silica has a 7 nm pore-size aperture (Figure S6a, Supporting Information). However, a uniform hexagonal array of pores with open-ended cylindrical mesoporous channels makes SBA-15 a much more confined matrix for sulfur impregnation rather than its carbon replica (Figure S6b, Supporting Information). Interestingly, prior to completing our study, Nazar et al. recently published a paper[21] on the electrochemical behavior of carbon−sulfur composite in the presence of 10% SBA-15 additives. The authors were inspired by early studies dealing with the use of triblock copolymer-templated SBA-15 as a reversible drug delivery system. As our results confirm their findings, we will briefly pass on the electrochemical performances of our electrodes prior to describing in more detail the specific analyses aiming to unravel the outcome of the polysulfides within these confined mesoporous oxides.

SBA-15/S composites were prepared under the same protocol previously described for MIL-100(Cr)/S composites, and according to TGA analysis, 52 wt % sulfur was successfully infiltrated into the pore matrix (data now shown). In contrast to the MOF, XPS analysis has revealed the absence of S-silica matrix interactions since there is no evolution of S2p BE observed for SBA-15/S@155 (Figure 3c), indicating that the presence of accessible transition-metal cation (Cr) in MIL-100 may be a key parameter. Additionally, the amount of S detected was well below the nominal one, implying that S was deeply impregnated within the core of the SBA particles. The Li storage properties of SBA-15 derived cathode composites are shown in Figure 2c and d. Here again, like it was observed with the MOF, we note an improvement in capacity retention as compared to mesoporous carbon/S composites due to a prominent sulfur impregnation into individual closed tubular channels of SBA-15 rather than its replicated carbon in which sulfur is located between a number of thick carbon nanorods (6−7 nm in diameter) assembled in a hexagonal arrangement (Figure S6b, Supporting Information). As for the MOF, this confirms the importance of adding mesoporous additives capable of adsorbing/desorbing the polysulfides. However, this improvement is still far from satisfactory, since we are unable to cycle S-based electrodes without having noticeable capacity degradation.

In order to highlight the structural benefit of MIL-100(Cr) and SBA-15, whose physical properties are summarized in Table 1, we monitored quantitatively the amount of polysulfide species in the electrolyte by means of in situ CV measurement with a homemade four-electrode cell at the first discharge, which has already proven to be a versatile tool to find a better environment for Li−S batteries.[22] Figure 4a, b, and c shows the first discharge curves of the MOF/S, mesoporous carbon/S, and SBA-15/S composites as well as their corresponding cumulative charges calculated from the integration of the peak between 2.25 and 1.5 V vs Li in CV measurements in Figure S7, Supporting Information, respectively. This measurement is performed at a slightly lower current density (C/20) than the galvanostatic measurements (C/10) in order to observe a pronounced polysulfide formation. Then after every 0.1e^- insertion, CV of the resultant species was applied. Measurements were repeated in this sequence until the battery reached the cutoff voltage of 1.0 V versus Li. From these experiments, we see that the total cumulative charge of the

MIL-100(Cr)/S@155 + 50%C (3.9 μAh) is much lower than that of mesoporous carbon/S@155 composite (10.8 μAh) as well as SBA-15)/S@155 + 50%C (9.2 μAh). These results are expected since the small size of the pore windows (5−8.6 Å) of the MIL-100(Cr) would lower the diffusion of the polysulfides from the matrix contrary to mesoporous carbon and silica. Additionally, considering the long-term cycling performances (Figure 4d), the capacity decay is much more flat in the case of MOF/S composite, which could be again linked to its pore shape.

In conclusion, we here demonstrated that the MIL-100(Cr) host, which combines a unique topology (large pore and small windows), a high chemical stability, and a balanced polar character, together with SBA-15, which belongs to the large family of mesoporous silica, is a suitable absorbing material for sulfur impregnation. Both insulating mesoporous MIL-100(Cr) and SBA-15 structures were found to be more efficient than the mesoporous carbon for the proper functioning of S electrodes, which is indicative of the greater importance of electrode confinement over electrode conductivity.

Table 1. Structural Properties of MIL-100(Cr), SBA-15, Mesoporous (MP) Carbon Calculated From N2 Sorption Analysis

	BET surface area ($m^2\ g^{-1}$)	mesoporous volume ($cm^3\ g^{-1}$)	pore size (nm)
MIL-100(Cr)	1485	0.95	2.5 (window <1)
SBA-15	740	0.85	7−9
MP carbon	1160	1.05	4.3

The importance of this confinement can be explained taking into account the functioning of a Li−S battery, which enlists the formation of soluble polysulfide species at the positive electrode. These species easily migrate out of the electrode toward the negative electrode where they are reduced to non soluble and insulating Li_2S species, hence leading to progressive capacity losses upon cycling. Thus, it does not come as a surprise that trapping the polysulfide species within the positive electrode improves the electrochemical performances of Li−S cells.

In contrast, the greater efficacy of insulating porous structures as compared to mesoporous carbon structures is at first counterintuitive and deserves some explanation, which mainly relies on the physics of capillarity. These porous host structures can be viewed as constituted of tubular-shape entities (e.g., pipes) capable of hosting sulfur and liquid (e.g., electrolyte). The filling of such tubes with either liquid sulfur or electrolyte is mainly driven by capillary effects, and the flow conditions within these tubes, whether they consist of carbon or oxide walls, depends upon numerous parameters among which is the dimension of the tubes together with the chemical nature of the tube walls.

Within our experiments, elemental sulfur is liquefied and mainly driven within the tubes by capillary forces. Once the S/host structure electrode is reduced within an electrochemical cell, there is a formation of soluble polysulfides which can migrate through the electrolyte. Such a migration is expected to depend upon the chemical/physical parameters pertaining to the host structures,

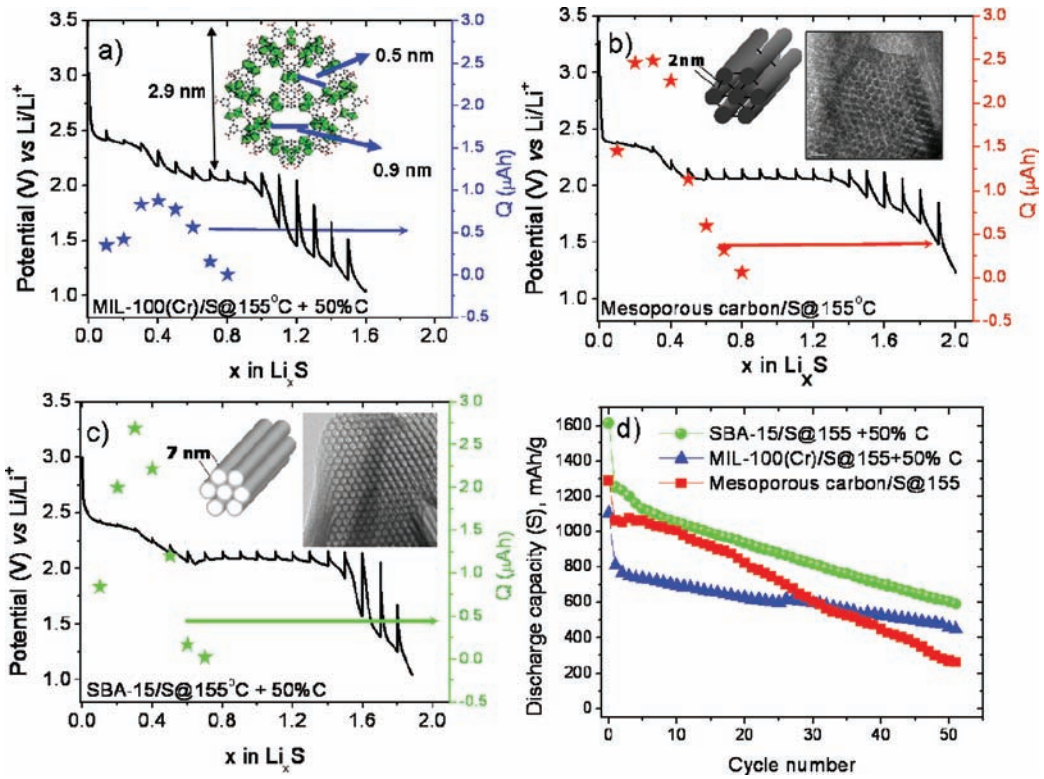

Figure 4. Electrochemical behavior during the first reduction of: (a) MIL-100(Cr)/S@155 + 50%C composite, (b) mesoporous carbon/sulfur@155, and (c) SBA-15/S@155 + 55%C composite in 1 M of LiTFSI in TMS electrolyte with C/20 current density for the voltage range between 1.0 and 3.0 V vs Li. Blue, red, and green stars present the partial cumulative charge obtained from the integration of the peak between 2.25 and 1.5 V in CV in Figure S7, Supporting Information. (d) Cycling performance of the composites in 1 M of LiTFSI in TMS electrolyte with C/10 current density for the voltage range between 1.0 and 3.0 V vs Li.

dx.doi.org/10.1021/ja2062659 |J. Am. Chem. Soc. 2011, 133, 16154–16160

namely the length and diameter of the pores together with the walls pore surface activity. The latter appears essential to explain our results. Both MOF and mesoporous silica additives present more polarized surfaces than C so that they are capable to interact strongly with charged species, such as Li_2S_x. Thus, one would expect the onset of such surface interactions between the host structures and polysulfides to slowdown the migration of the polysulfide species. Hence, a better capacity retention of both silica and MOF loaded composite electrodes as compared to the mesoporous carbon ones should result. Purely coincidentally or not, this is what we experimentally observed.

Aside from the O−S surface interactions, another point to elucidate deals with the feasibility of triggering the electrochemically activity of S located at the inner side of tubes cores having insulating walls surrounded by a carbon conducting matrix. We are here mimicking an insulator−metal junction, whose physics has been well studied, with the possibility of having electrons tunneling through the insulating layer, if its thickness is of the order of several nanometers, depending upon the nature of the insulating material. The pore wall thickness is composed of a single layer of atoms for MIL-100(Cr) host (thus a thickness <1 nm), and for SBA-15 structures, it is the order of a few nanometers, we believe that electron tunneling can take place then providing some electronic conductivity at the internal surface of the pore wall so that electrochemical reaction, which necessitates both electrons and ions at the same location, can take place. Needless to say that a threshold amount of carbon matrix (25%) as experimentally proved is necessary to serve as conducting matrix. Initial experiments with a copper-based MOF show that these materials reversibly cycle lithium without degrading the MOF structure. The materials are electronically conducting, with the redox kinetics improved by adding carbon to the MOF electrode.[23]

Although our understanding of the MOF−S composite electrode functioning is still very sketchy, we believe that in the field of Li−S batteries, the design of electrodes with a high degree of confinement obtained by using mesoporous MOFs, zeolites, or even carbon structures to host elemental sulfur is essential for enhancing the cycle life of Li−S batteries. Aside from this confinement effect, the surface activity of the mesoporous additives appears to also have a pronounced effect. To get further insight into this comparative surface activity between MOF, silica, and mesoporous carbon-based matrices carbide-derived carbons (CDC),[24] whose uniform pore sizes can be nicely tailored to values ranging from 0.5 to about 6 nm depending upon the synthesis conditions, present studies are ongoing together with grafting investigation of various molecules to tune the S-host interaction. Besides a wide variety of nanostructured confined matrixes, beyond those reported here, remains to be found and chemically adjusted to be used as efficient host positive electrode support for Li/S batteries. Will such a new approach be sufficient for the Li/S technology that has been around for a few decades? This remains to be seen.

■ ASSOCIATED CONTENT

Supporting Information. Supporting figures and resulting references. This material is available free of charge via the Internet at http://pubs.acs.org.

■ AUTHOR INFORMATION

Corresponding Author
jean-marie.tarascon@sc.u-picardie.fr.

■ ACKNOWLEDGMENT

The authors acknowledge the ANR 'CONDMOFs' project and ALISTORE European Research Institutive (ERI) for the financial support. M. Courty (UPJV, Amiens) is warmly thanked for the DSC and TGA-DTA experiments.

■ REFERENCES

(1) Herbert, D.; Ulam, J. U.S. Patent, 3 043 896, 1962.
(2) Armand, M.; Tarascon, J.-M. *Nature* **2008**, *451*, 652.
(3) Yamin, H.; Gorenshtein, A.; Penciner, J.; Stenberg, Y.; Peled, E. J. *Electrochem. Soc.* **1988**, 1045.
(4) Aurbach, D.; Pollak, E.; Elazari, R.; Salitra, G.; Kelley, G. S.; Affinito, J. J. *Electrochem. Soc.* **2009**, *156*, A694.
(5) Jeong, S. S.; Lim, Y. T.; Choi, J. Y.; Kim, G. B.; Ahn, H. J.; Cho, K. K. *J. Power Sources* **2007**, *174*, 745.
(6) Ji, X.; Lee, K. T.; Nazar, L. F. *Nat. Mater.* **2009**, *8*, 500.
(7) Ferey, G.; Millange, F.; Morcrette, M.; Serre, C.; Doublet, M.-L.; Greneche, J.-M.; Tarascon, J.-M. *Angew. Chem. In. Ed.* **2007**, *46*, 3259.
(8) Nguyen, T. L. A.; Demir-Cakan, R.; Devic, T.; Morcrette, M.; Ahnfeldt, T.; Auban-Senzier, P.; Stock, N.; Goncalves, A.-M.; Filinchuk, Y.; Tarascon, J.-M.; Ferey, G. *Inorg. Chem.* **2010**, *49*, 10710.
(9) de Combarieu, G.; Morcrette, M.; Millange, F.; Guillou, N.; Cabana, J.; Grey, C. P.; Margiolaki, I.; Ferey, G.; Tarascon, J.-M. *Chem. Mater.* **2009**, *21*, 1602.
(10) Meilikhov, M.; Yusenko, K.; Esken, D.; Turner, S.; Van Tendeloo, G.; Fischer, R. A. *Eur. J. Inorg. Chem.* **2010**, 3701 and references therein.
(11) Müller, M.; Zhnag, X.; Wang, Y.; Fischer, R. A. *Chem. Commun.* **2009**, 119.
(12) Bhakta, R. K.; Herberg, J. L.; Jacobs, B.; Highley, A.; Behrens, R., Jr.; Ockwig, N. W.; Greathouse, J. A.; Allendorf, M. D. *J. Am. Chem. Soc.* **2009**, *131*, 13198.
(13) McKinlay, A. C.; Morris, R. E.; Horcajada, P.; Ferey, G.; Gref, R.; Couvreur, P.; Serre, C. *Angew. Chem., Int. Ed.* **2010**, *49*, 6260and references therein.
(14) Low, J. J.; Benin, A. I.; Jacubczak, P.; Abrahamian, J. F.; Faheem, S. A.; Willis, R. R. *J. Am. Chem. Soc.* **2009**, *131*, 15934.
(15) Cychosz, K. A.; Matzger, A. J. *Langmuir* **2010**, *26*, 17198.
(16) Ferey, G.; Serre, C.; Mellot-Draznieks, C.; Millange, F.; Surble, S.; Dutour, J.; Margiolaki, I. *Angew. Chem., Int. Ed.* **2004**, *43*, 6296.
(17) Hamon, L.; Serre, C.; Devic, T.; Loiseau, T.; Millange, F.; Férey, G.; De Weireld, G. *J. Am. Chem. Soc.* **2009**, *131*, 8775.
(18) Ravet, J. B. G. N.; Besner, S.; Simoneau, M.; Hovington, P.; Armand, M. Proceedings of The Electrochemical Society and the Electrochemical Society of Japan Meeting October, Vienna, Austria, October 4−9, 2009; The Electrochemical Society: Pennington, NJ, 1999.
(19) Dominko, R.; Gaberscek, M.; Drofenik, J.; Bele, M.; Pejovnik, S.; Jamnik, J. *J. Power Sources* **2003**, *19*−*121*, 770.
(20) Zhao, D.; Huo, Q.; Feng, J.; Chmelka, B. F.; Stucky, G. D. *J. Am. Chem. Soc.* **1998**, *120*, 6024.
(21) Ji, X.; Evers, S.; Black, R.; Nazar, L. F. *Nature Comm*, **2011**, DOI: 10.1038/ncomms1293.
(22) Dominko, R.; Demir-Cakan, R.; Morcrette, M.; Tarascon, J. M. *Electrochem. Commun.* **2011**, *13*, 117.
(23) Bruce Dunn et al. private communication
(24) Chmiola, J.; Yushin, G.; Gogotsi, Y.; Portet, C.; Taberna, P. L.; Simon, P. *Science* **2006**, *313*, 1760.